



Published in final edited form as:

Acc Chem Res. 2016 August 16; 49(8): 1494–1502. doi:10.1021/acs.accounts.6b00210.

## Live-cell bioorthogonal chemical imaging: stimulated Raman scattering microscopy of vibrational probes

Lu Wei<sup>1</sup>, Fanghao Hu<sup>1</sup>, Zhixing Chen<sup>1</sup>, Yihui Shen<sup>1</sup>, Luyuan Zhang<sup>1</sup>, and Wei Min<sup>1,2,\*</sup>

<sup>1</sup>Department of Chemistry, Columbia University, New York, 10027

<sup>2</sup>Kavli Institute for Brain Science, Columbia University, New York, 10027

### Conspectus

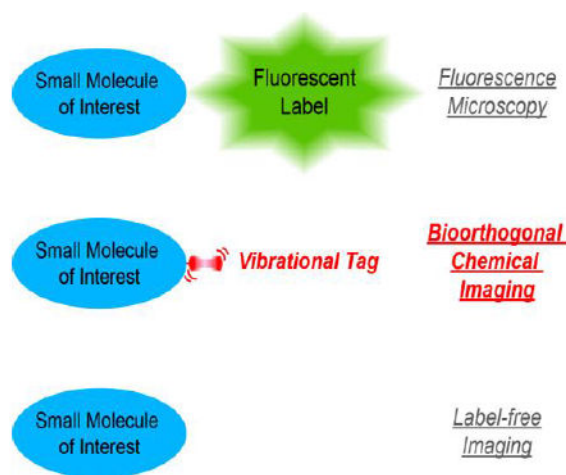
Innovations in light microscopy have tremendously revolutionized the way researchers study biological systems with subcellular resolution. In particular, fluorescence microscopy with the expanding choices of fluorescent probes has provided a comprehensive toolkit to tag and visualize various molecules of interest with exquisite specificity and high sensitivity. Although fluorescence microscopy is currently the method of choice for cellular imaging, it faces fundamental limitations for studying the vast number of small biomolecules. This is because that common fluorescent labels, which are relatively bulky, could introduce considerable perturbation to or even completely alter the native functions of vital small biomolecules. Hence, despite their immense functional importance, these small biomolecules remain largely undetectable by fluorescence microscopy.

To address this challenge, a *Bioorthogonal Chemical Imaging* platform has recently been introduced. By coupling the stimulated Raman scattering (SRS) microscopy, an emerging nonlinear Raman microscopy technique, with tiny and Raman-active vibrational probes (e. g. alkynes and stable isotopes), *Bioorthogonal Chemical Imaging* exhibits superb sensitivity, specificity and biocompatibility for imaging small biomolecules in live systems. In this Account, we review recent technical achievements for visualizing a broad spectrum of small biomolecules, including ribonucleosides/deoxyribonucleosides, amino acids, fatty acids, choline, glucose, cholesterol and small-molecule drugs in live biological systems ranging from individual cells to animal tissues and to model organisms. Importantly, this platform is compatible with live-cell biology, thus allowing real-time imaging of small-molecule dynamics. Moreover, we discuss further chemical and spectroscopic strategies for *multicolor Bioorthogonal Chemical Imaging*, a valuable technique in the era of “omics”.

As a unique tool for biological discovery, this platform has been applied to studying various metabolic processes under both physiological and pathological states, including protein synthesis activity of neuronal systems, protein aggregations in Huntington disease models, glucose uptake in tumor xenograft and drug penetration through skin tissues. We envision that the coupling of SRS microscopy with vibrational probes would do for small biomolecules what fluorescence microscopy of fluorophore has done for larger molecular species.

### Graphical abstract

\*Corresponding author. wm2256@columbia.edu.



## 1. INTRODUCTION

Light microscopy, in particular, the fluorescence microscopy has been a powerful tool for researchers to study living systems at the microscopic level<sup>1,2</sup>. However, there remains a fundamental limitation for fluorescence imaging of small biomolecules, such as nucleosides, amino acids, fatty acids, choline, glucose, cholesterol and small-molecule drugs in living systems. **This is because most of small biomolecules are intrinsically non-fluorescent.**

However, fluorescent probes such as organic dyes, fluorescent proteins or quantum dots are all relatively bulkier in size than small biomolecules, thus often severely compromising the native biochemical or biophysical properties of these fluorophore-labeled small biomolecules inside live cells. Therefore, optical imaging methods offering molecular contrasts other than fluorescence are needed to study these small chemical species.

Raman microscopy presents an alternative for this purpose. Based on vibrational spectroscopy without the need of bulky fluorophore labeling, Raman imaging holds the promise for probing small molecules<sup>3</sup>. However, the spontaneous Raman scattering (Figure 1a) is notoriously feeble, which needs long acquisition time and is vulnerable to sample auto-fluorescence. As a result, conventional Raman microscopy is a less-than-ideal bio-imaging modality, especially for **applications demanding high sensitivity, fast speed, deep tissue penetration or correlative fluorescence and Raman imaging**<sup>4,5</sup>. An advanced Raman technique, **Surface Enhanced Raman Scattering (SERS)**, could provide much higher sensitivity. **Nevertheless, its reliance on metallic nanostructures limits its ability to probe small intracellular biomolecules**<sup>6</sup>.

Partially overcoming both the sensitivity and biocompatibility issues, coherent anti-Stokes Raman scattering (CARS) microscopy offers an imaging speed close to fluorescence microscopy by virtue of coherent amplification (Figure 1a)<sup>7</sup>. **Unfortunately, CARS microscopy suffers from spectral distortion, unwanted nonresonant background and non-straightforward concentration dependence**<sup>8,9</sup>. Although some of these limitations can be addressed by advanced CARS derivatives, substantial technical complexity has to be involved<sup>8,10</sup>.

More recently, stimulated Raman scattering (SRS) microscopy emerged to complement and even supersede CARS in almost all aspects (Figure 1a)<sup>11-17</sup>. Spectroscopically, the SRS spectrum is identical to that of spontaneous Raman without the complication of non-resonant background, thus offering straightforward and robust spectral interpretations<sup>12,18</sup>. The detection sensitivity of SRS readily approaches the shot-noise limit by taking advantage of the high-frequency modulation transfer scheme<sup>15,17</sup>. In addition, SRS signals are strictly linear dependent on analyte concentrations, allowing for quantitative analysis. Moreover, the nonlinear nature and the adoption of near-infrared laser wavelengths allow SRS 3D optical sectioning into deep tissues.

In the most popular narrow-band excitation scheme, SRS microscopy utilizes two spatially and temporally synchronized picosecond laser pulse trains (pump and Stokes)<sup>12, 14-17</sup>. When the energy gap between two lasers is resonant with the vibrational level of targeted chemical bonds, the joint action of the pump and Stokes fields stimulates (i.e., accelerates) the otherwise slow vibrational transition by  $10^8$  times<sup>15,17</sup>. Whenever a molecule is promoted into the vibrational excited state, the Stokes pulse gains a photon, whereas the pump pulse loses one (Figure 1b). By modulating the Stokes beam (or the pump beam) intensity at a high frequency ( $\sim$ MHz) and detecting the resulting stimulated Raman loss (or gain) of the pump beam (or the Stokes beam) with a photodiode fed to a lock-in amplifier referenced at the same frequency as the modulation, shot-noise-limited high detection sensitivity is achieved, circumventing the laser intensity fluctuations occurring at low frequencies<sup>12,15</sup> (Figure 1b). After raster-scanning across the sample, one can produce a 3D concentration map of the targeted chemical bonds.

## 2. LABEL-FREE CHEMICAL IMAGING

Since the invention of the narrow-band SRS microscopy<sup>12</sup>, label-free imaging has been a central theme of its applications. A variety of molecular species have been imaged by label-free SRS targeting their intrinsic chemical bonds at the crowded cellular fingerprint region ( $500\text{-}1700\text{ cm}^{-1}$ ) or the high frequency C-H or O-H region ( $2800\text{-}3200\text{ cm}^{-1}$ ). Chemical bonds frequently probed are O-P-O, N-C=O, C=C, S=O, O-H, C-H<sub>2</sub>, C-H<sub>3</sub> (Figure 1c). Notable examples include (but not limited to) monitoring DMSO and retinoic acid diffusion through skins of living mice and human<sup>12</sup>, video-rate imaging for skin samples<sup>14</sup>, imaging nucleic acids *in vivo*<sup>19</sup>, delineating tumor margins<sup>20</sup>, tracking changes of lipid composition<sup>21</sup>, imaging intracellular drug distribution in living cells<sup>22</sup> and detecting membrane potential<sup>23</sup>. The success of these label-free applications has inspired the developments for spectroscopic imaging and will continue to generate a profound impact in biomedicine<sup>17</sup>.

Despite the popularity of label-free imaging for biomedicine, this strategy has a few limitations. First, the detection specificity is usually compromised. It is rather difficult to distinguish a target biomolecule from the sea of the other related species inside cells since the differentiable vibrational signatures are finite and many bio-molecular species share similar chemical bonds<sup>24</sup>. Second, the Raman scattering cross-sections of the endogenous chemical bonds are usually limited. The resulting detection sensitivity of label-free SRS is often in the range of mM, not sensitive enough for capturing the activities of many

同一团细胞可能出现相近的化学键 => label-free 准确率受到影响

Raman 散射范围不够小, 导致没法检测很多小分子

interesting small biomolecules<sup>15</sup>. Third, although label-free approach is highly powerful for stationary imaging, it usually lacks the ability for probing dynamic metabolism including uptake, trafficking, and turnover of small biomolecules. Therefore, there is a strong need for conceptual innovations to go beyond the label-free strategy to further boost specificity and sensitivity, as well as to probe dynamics.

缺少动态捕捉的能力

### 3. BIOORTHOGONAL CHEMICAL IMAGING: SRS MICROSCOPY OF VIBRATIONAL PROBES

The concept of vibrational probes has been around in the field of vibrational spectroscopy<sup>25</sup>. Indeed, nitriles ( $C\equiv N$ ) and carbonyls ( $C=O$ ) are used to probe local electrostatics and dynamics in proteins and enzymes through the vibrational Stark effect<sup>26</sup>. Evolving from spectroscopy to microscopy, the idea of detecting vibrational probes leads to the initial demonstrations of spontaneous Raman imaging of Raman active probes including stable isotopes (Huang et al.<sup>27</sup> and van Manen et al.<sup>28</sup>) and alkynes, i.e.  $C\equiv C$ , (Yamakoshi et al.<sup>29, 30</sup>) inside cells and SERS imaging of bioorthogonal Raman reporter on cell surface (Lin et al.<sup>31</sup>). Among the probes, alkynes stand out as widely exploited small molecule handles for imaging and identification in the booming field of *Bioorthogonal Chemistry*<sup>32-38</sup>. Inspired by these previous efforts and success, a general *Bioorthogonal Chemical Imaging* platform has recently emerged by coupling SRS microscopy with tiny vibrational probes<sup>39-50</sup>. Such an optical imaging scheme presents a hybrid strategy between the conventional fluorescence microscopy and the label-free vibrational imaging approach, thereby offering the desired combination of high detection sensitivity and specificity, minimal perturbations and dynamical analysis capacity.

Specifically, three distinct classes of bioorthogonal vibrational probes were explored: alkyne ( $C\equiv C$ ) moieties, deuterium isotope and  $^{13}C$  isotope. Physically, unlike the bulky fluorophores, these probes consist of only several atoms, thus exerting little perturbation to the native function of small biomolecules. Spectroscopically, both  $C\equiv C$  (as well as  $C\equiv N$ ) and deuterium isotope exhibit Raman peaks at the cell-silent region where no other peaks from endogenous molecules exist (Figure 1c), achieving exquisite detection specificity. Biochemically, these probes are generally absent (or at extremely low abundance) inside cells, and are inert to cellular reactions or exchanges. Hence, SRS imaging of these vibrational probes, which are both spectroscopically and biochemically orthogonal to the endogenous molecules inside cells, is termed *Bioorthogonal Chemical Imaging*. Such a platform is well suited for probing small-molecule dynamics in living systems with high spatial and temporal resolution. We herein summarize and discuss the most recent advances toward this front.

### 4. SRS IMAGING OF ALKYNES FOR VISUALIZING SMALL BIOMOLECULES WITH HIGH SENSITIVITY

Alkynes possess desirable features for tagging a wide variety of small biomolecules with subsequent imaging by SRS microscopy. Chemically, they are small (only two atoms), bioorthogonal and easy to be installed<sup>32-38</sup>. Spectroscopically, the stretching motion of  $C\equiv C$

presents a substantial change of polarizability, displaying a sharp and strong Raman peak around 2125 cm<sup>-1</sup> in the cell-silent region<sup>24</sup>. In fact, Raman scattering cross-sections of alkynes are higher than almost all the endogenous chemical bonds in label-free imaging. The reported SRS detection limit for alkynes is down to 200 μM under a 100 μs acquisition time in 5-ethynyl-2'-deoxyuridine (EdU), an alkyne-tagged thymidine analog<sup>39</sup>, much more sensitive than previous label-free SRS reports in the mM range<sup>12</sup>.

Although alkynes have been heavily explored as imaging and identification handles in *Bioorthogonal Chemistry*<sup>32-38</sup>, clearly proving their minimal toxicity and high biocompatibility *in vivo*, the subsequent visualization by click-reaction between alkyne-tagged molecules and azide-tagged fluorophores normally involves the catalysis of copper(I) ion which is toxic to live cells. Even for the latest copper-free version, the reaction has non-ideal kinetics and is often associated with high background originated from nonspecific staining<sup>51</sup>. Moreover, it is a non-trivial task to homogeneously deliver these fluorophores to live tissues and animals. To this end, direct SRS imaging of alkyne-tagged small molecules is free from all these complications by bypassing the click reaction and the fluorophores altogether.

Wei *et al.* in 2014 first demonstrated SRS imaging for a broad spectrum of alkyne-tagged small-molecule building blocks, including deoxyribonucleosides, ribonucleosides, amino acids, choline and fatty acids (Figure 2a) for the *de novo* synthesis of DNA, RNA, proteome, phospholipids and triglycerides (Figure 2b, c)<sup>39</sup>. Shortly afterwards, Hong *et al.* reported similar applications with an additional alkyne-tagged glycan<sup>40</sup>. In addition to small-molecule building blocks, Hu *et al.* recently synthesized and evaluated alkyne-tagged glucose (Figure 2a, b) as an important metabolic probe for interrogating energy demands in live cells and tissues (Figure 2c), and observed heterogeneous glucose uptake patterns with clear cell-to-cell variations in tumor xenograft tissues<sup>41</sup>.

Small-molecule drugs represent an important class of targets for *Bioorthogonal Chemical Imaging*, since there has been a lack of non-perturbative imaging technologies with high sensitivity and specificity as well as fine spatial and temporal resolution. SRS imaging of alkyne-tagged small-molecule drugs has proven to be effective by evaluating the pharmacokinetics of Terbinafine Hydrochloride (TH), a FDA approved antifungal drug (Figure 3a)<sup>39</sup>. Taking advantage of the deep-tissue imaging capability of SRS, the drug penetration patterns after topically applied to mouse ear tissues were revealed. The TH images captured at different depths were all found to highly resemble the lipid but not the protein distributions in the tissues (Figure 3b), suggesting that TH penetrates into tissues through the lipid phase, consistent with its lipophilic nature<sup>39</sup>. This demonstration suggests that SRS tracking of alkyne probes could be a general method for drug imaging after proper alkyne derivatization.

The conjugation system of alkynes can also be slightly enlarged to gain higher SRS signals in a case-by-case manner. Along this line, Lee *et al.* used SRS imaging of phenyl-diyne tagged cholesterol to assess cholesterol storage in live cells and *C. elegans*<sup>42</sup>, in which phenyl-diyne is found to exhibit an about 5-time higher signal than a single alkyne in EdU<sup>39,42</sup>. Very recently, Ando *et al.* synthesized a diyne-tagged sphingomyelin analog, and

alkynes的不足之处

1: 需要铜离子参与到反应中, 会对人体造成伤害, 无法做in vivo实验

2: 探针的均一化部署有困难

Application

observed a heterogeneous spatial distribution of this probe within *in vitro* raft-like ordered domains by spontaneous Raman<sup>52</sup>. In these cases, the trade-off between the probe size and the achievable SRS signals needs to be carefully balanced.

## 5. SRS IMAGING OF ISOTOPE LABELS

Although alkyne tagging has been proven to be effective and generally applicable, the chemical modifications inevitably introduce a variable degree of alteration to the rates of biosynthesis and metabolism for the tagged biomolecules compared to their natural counterparts. For example, cells incorporate Hpg (homopropargylglycine), an alkyne-bearing Methionine (Met) analogue, about 500 times slower than Met<sup>34</sup>. In this regard, stable isotopes (e.g. deuterium and C<sup>13</sup>) emerge as better vibrational probes, since they only differ to their natural counterparts by neutron numbers and thus closely mimicking the corresponding physicochemical properties.

### 5. 1. Carbon-deuterium probes (C-D)

Carbon-deuterium bonds (C-D) are a type of particularly suited vibrational probes. Chemically, deuterium is the stable isotope of hydrogen without any radioactivity and has an extremely low natural abundance (~0.016%). Thus, replacing the naturally occurring carbon-hydrogen bonds (C-H) with C-D introduces stable labels with minimum physicochemical alterations. As a matter of fact, the FDA is considering a first approval of a deuterated drug<sup>53</sup>. The kinetic isotope effect is usually negligible for the incorporation and imaging duration of typical experiments. Spectroscopically, C-D also display Raman peaks centered around 2100 cm<sup>-1</sup> in the desired cell-silent spectral region, shifting the vibrational frequency,  $\Omega_{vib}$ , away from that of C-H by modulating the reduced mass,  $\mu$ , in the classical mechanics equation  $\Omega_{vib} \propto \sqrt{k/\mu}$ . Hence it is not surprising that C-D have been harnessed by Raman spectroscopists and microscopists for decades.

Earlier SRS microscopy of C-D has been convincingly demonstrated for tracking deuterated DMSO penetration in skin tissues and for imaging cellular uptake of deuterated fatty acids<sup>12, 44</sup>. In 2013 Wei *et al.* reported that C-D are especially suitable for tagging amino acids on the stable side-chains and for subsequent SRS imaging of protein synthesis activities<sup>45</sup>. Although the Raman cross-section of C-D is about 30-40 times lower than alkynes<sup>30,39</sup>, the particular setting of labeling amino acids by C-D is more ideal, thanks to the enormous number of stable C-H (up to ~ Molar in concentration) in multiple amino acids that make up proteins.

*De novo* protein synthesis is the last step of the central dogma, responsible for the basic cell survival and proliferation and various cellular responses to environmental stimuli. For instance, this process is closely related to the long-term memory formation in neuroscience<sup>54,55</sup>. When deuterated amino acids (D-AAAs) are supplied to the cell growth medium, they will be metabolically incorporated by cells' natural translational machineries as essential building blocks into newly synthesized proteins (Figure 4a)<sup>45</sup>. Therefore, sensitive and specific SRS imaging of newly synthesized proteins enriched with C-D can be achieved by targeting the unique vibrational signature of C-D<sup>45</sup>. As a contrast, the un-



incorporated D-AAs in the free amino acid pool are too dilute to be detected. Because of such high signals and bio-compatibility offered by D-AA labeling, high-quality SRS imaging of protein synthesis has been demonstrated ranging from live mammalian cells, neurons, to live brain tissues, and to zebrafish and mice *in vivo* (Figure 4b)<sup>45,46</sup>. Particularly, fast mapping of protein synthesis activities has been achieved across a large-area brain tissue (4 mm-by-3 mm) within only 2.2 min<sup>46</sup>. Such valuable information of when and where new proteins are actively synthesized in living systems is hard to obtain by other means, such as stable isotope labeling by amino acids in cell culture coupled with mass spectrometry (SILAC-MS)<sup>56</sup>.

Moving beyond fatty acids and amino acids, very recently, Hu *et al.* used D9-choline for imaging choline metabolism in live cells and *C. elegans*<sup>47</sup>, Li *et al.* implemented D7-glucose for tracing *de novo* lipogenesis<sup>48</sup>, and Alfonso-García *et al.* adopted D38-cholesterol to assess intracellular cholesterol storage<sup>49</sup>. All these applications prove the universal effectiveness and the superb biocompatibility of SRS imaging with C-D tagging.

## 5. 2. <sup>13</sup>C probe

<sup>13</sup>C could also serve as an effective bioorthogonal probe due to its low natural abundance (~1.109%) and its ability to shift the vibrational frequency from the <sup>12</sup>C counterparts. Indeed, <sup>13</sup>C-tagged metabolites have been used in spontaneous Raman for probing cell metabolism<sup>27,57</sup>. Coupling with SRS microscopy, Shen *et al.* recently demonstrated that <sup>13</sup>C-tagged phenylalanine for quantitative imaging of proteome degradation<sup>50</sup>. By employing the characteristic ring-breathing modes of endogenous <sup>12</sup>C-Phenylalanine (<sup>12</sup>C-Phe) at 1004 cm<sup>-1</sup> and the metabolically incorporated <sup>13</sup>C-Phe at 968 cm<sup>-1</sup> as the spectroscopic markers for the old and new proteome, respectively, proteomic degradation can be imaged by SRS in living cells by ratio maps of <sup>12</sup>C/(<sup>12</sup>C+<sup>13</sup>C), in which the total proteome is represented by the sum of <sup>12</sup>C-Phe and <sup>13</sup>C-Phe (Figure 5)<sup>50</sup>.

Proteome degradation is a key process to regulate cellular response under pathological or dysfunctional states<sup>58</sup>. Shen *et al.* applied the method to study the impact of protein aggregation on proteomic degradation of mutant huntingtin proteins in a mammalian cell model<sup>50</sup>. The obtained results from correlative SRS microscopy and fluorescence imaging of GFP-labeled huntingtin support the emerging hypothesis that while the diffusive oligomers of aggregation-prone proteins might be toxic by gradually interfering with the proteasome machinery, the formation of inclusion bodies could be neuroprotective by sequestering the diffusive toxic species<sup>59</sup>.

## 6. FUNCTIONAL IMAGING OF DYNAMIC SMALL-MOLECULE METABOLISM IN LIVE SYSTEMS

A distinguished advantage for the *Bioorthogonal Chemical Imaging* platform is its superb biocompatibility. Therefore, real-time dynamic analysis is achievable by SRS imaging of vibrational probes to track the intracellular fates of small biomolecule in live systems. Such a capability is beyond the reach of competing techniques, such as click-chemistry followed with fluorescence visualization<sup>32-38, 51</sup>, SILAC-MS<sup>56</sup> and multi-isotope imaging mass

spectrometry<sup>60</sup>. To this end, Wei *et al.* demonstrated the dynamic tracking of cell division after incorporation with either EdU into newly synthesized DNA (Figure 6a)<sup>39</sup> or D-AAs into new proteome (Figure 6b)<sup>45</sup>. In addition, time-lapse imaging from 10 min to 5 h of active *de novo* protein synthesis on the same set of mammalian cells were also shown (Figure 6c)<sup>46</sup>.

## 7. MULTI-COLOR BIOORTHOGONAL CHEMICAL IMAGING

A recurring and powerful theme in fluorescence microscopy is the creation of a fluorescent palette, enabling multicolor analysis for separation, co-localization and interactions. Inspired by the success of fluorescent palettes, a vibrational palette for multicolor *Bioorthogonal Chemical Imaging* of small biomolecules has also been created. Chen *et al.* reported isotopic edition of alkynes by modulating the reduced mass of the triple bonds<sup>43</sup>. The resulting vibrational frequencies  $\Omega_{vib}$  are shifted from  $\sim 2125\text{ cm}^{-1}$  of the original  $\text{C}\equiv\text{C}$  bond to  $2077\text{ cm}^{-1}$  of  $^{13}\text{C}\equiv\text{C}$  and to  $2053\text{ cm}^{-1}$  of  $^{13}\text{C}\equiv^{13}\text{C}$ . With this novel vibrational palette, previously non-differentiable small biomolecules bearing the same alkynes could now be spectrally separated and imaged simultaneously (Figure 7a)<sup>43</sup>, paving the way for multiplex chemical imaging. Since triple bonds present an inherent narrow Raman peak ( $\sim 14\text{ cm}^{-1}$ ) and the cell-silent spectral window is rather wide ( $\sim 1700\text{--}2800\text{ cm}^{-1}$ ), we envision many more vibrational colors could be created upon further chemical manipulations.

In addition to multicolor SRS imaging of isotopic alkynes, Wei *et al.* performed two-color pulse-chase proteome imaging with D-AAs by rationally dividing all D-AAs with analogous chemical structures into two sub-groups. Using this method, aggregation formation of mutant huntingtin proteins was studied by pulse-chase labeling and imaging (Figure 7b, c)<sup>46</sup>, demonstrating the readily applicability of the method to untangle complex and dynamic aspect of proteome metabolisms. These vibrational palettes created by chemical editing and spectroscopic re-grouping empower *Bioorthogonal Chemical Imaging* a more versatile platform, allowing for comprehensive study of small biomolecules.

## 8. SUMMARY AND OUTLOOK

SRS microscopy was invented almost a decade ago. These passing years have witnessed the booming advances of SRS microscopy from instrumental developments to biomedical applications. Technically, fast and hyper-spectral SRS imaging modalities have been developed by several groups<sup>61-63</sup>. Biomedically, SRS imaging was applied to various studies such as successful delineation of tumor margins<sup>20</sup>. What was relatively lagging behind for the further developments of SRS imaging platform, however, is the contribution from chemistry to create more sensitive and versatile vibrational probes. To this end, we believe the chemical installments of vibrational probes to small biomolecules bridge such a gap between physics/engineering and biomedicine in a timely manner. In retrospect, this evolution path also echoes with the advance of fluorescence microscopy where the imaging probe development gradually becomes the center of the stage and drives innovation forward.

We anticipate the future development for *Bioorthogonal Chemical Imaging* platform in several fronts. First, chemical derivatization of alkynes (or nitriles) could be expanded to



more small biomolecules, such as neurotransmitters, co-enzymes and secondary messengers. Moreover, we expect this platform could be applied to interrogate and potentially offer new biological insights about more complex biological processes including tumor metabolism, long-term memory formation and neurodegenerative diseases in which the involvement of small molecule metabolism is critical yet hard to study, especially by fluorescence microscopy. Third, thanks to the high non-toxicity of stable isotope labeling, therapeutic imaging and clinical diagnostics, such as intraoperative tumor detection *in vivo* or even to human, could be expected in the near future.

## Acknowledgments

We appreciate helpful discussions with Meng Wang, Colin Nuckolls, Louis Brus, Ann McDermott, Ronald Breslow, Virginia Cornish, Rafael Yuste, Sunney Xie and Steven Boxer. This work is supported by NIH Director's New Innovator Award (1DP2EB016573), R01 (EB020892), the US Army Research Office (W911NF-12-1-0594), the Alfred P. Sloan Foundation and the Camille and Henry Dreyfus Foundation. Y. Shen acknowledges support from HHMI International Student Research Fellowship. Columbia University has filed a patent application based on this work.

## References

1. Pawley, JB., editor. Handbook of biological confocal microscopy. Springer; New York: 2006.
2. Yuste, R., editor. Imaging: a laboratory manual. Cold Spring Harbor Press; 2010.
3. Sasic, S., Ozaki, Y., editors. Raman, infrared, and near-infrared chemical imaging. Wiley; New York: 2011.
4. Suhaimi JL, Boik JC, Tromberg BJ, Potma EO. The need for speed. J Biophotonics. 2012; 5:387–395. [PubMed: 22344721]
5. Krafft C, Schie IW, Meyer T, Schmitt M, Popp J. Developments in spontaneous and coherent Raman scattering microscopic imaging for biomedical applications. Chem Soc Rev. 2016; 45:1819–1849. [PubMed: 26497570]
6. Lane LA, Qian X, Nie S. SERS nanoparticles in medicine: from label-free detection to spectroscopic tagging. Chem Rev. 2015; 115:10489–10529. [PubMed: 26313254]
7. Zumbusch A, Holtom GR, Xie XS. Three-dimensional vibrational imaging by coherent anti-Stokes Raman scattering. Phys Rev Lett. 1999; 82:4142–4145.
8. Evans CL, Xie XS. Coherent anti-Stokes Raman scattering microscopy: chemical imaging for biology and medicine. Annu Rev Anal Chem. 2008; 1:883–909.
9. Pezacki JP, Blake JA, Danielson DC, Kennedy DC, Lyn RK, Singaravelu R. Chemical contrast for imaging living systems: molecular vibrations drive CARS microscopy. Nat Chem Biol. 2011; 7:137–145. [PubMed: 21321552]
10. Camp CH Jr, Cicerone MT. Chemically sensitive bioimaging with coherent Raman scattering. Nature Photonics. 2015; 9:295–305.
11. Ploetz E, Laimgruber S, Berner S, Zinth W, Gilch P. Femtosecond stimulated Raman microscopy. Appl Phys B. 2007; 87:389–393.
12. Freudiger CW, Min W, Saar BG, Lu S, Holtom GR, He C, Tsai JC, Kang JX, Xie XS. Label-free biomedical imaging with high sensitivity by stimulated Raman scattering microscopy. Science. 2008; 322:1857–1861. [PubMed: 19095943]
13. Nandakumar P, Kovalev A, Volkmer A. Vibrational imaging based on stimulated Raman scattering microscopy. New J Phys. 2009; 11:033026.
14. Saar BG, Freudiger CW, Reichman J, Stanley CM, Holtom GR, Xie XS. Video-rate molecular imaging in vivo with stimulated Raman scattering. Science. 2010; 330:1368–1370.
15. Min W, Freudiger CW, Lu S, Xie XS. Coherent nonlinear optical imaging: beyond fluorescence microscopy. Annu Rev Phys Chem. 2011; 62:507–530. [PubMed: 21453061]
16. Cheng, J-X., Xie, XS. Coherent Raman Scattering Microscopy. CRC Press; Boca Raton, FL: 2013.

17. Cheng J-X, Xie SX. Vibrational spectroscopic imaging of living systems: emerging platform for biology and medicine. *Science*. 2015; 350:aaa8870. [PubMed: 26612955]
18. Kukura P, McCamant DW, Mathies RA. Femtosecond stimulated Raman spectroscopy. *Annu Rev Phys Chem*. 2007; 58:461–488. [PubMed: 17105414]
19. Lu F-K, Basu S, Igras V, Hoang MP, Ji M, Fu D, Holtom GR, Neel VA, Freudiger CW, Fisher DE, Xie XS. Label-free DNA imaging in vivo with stimulated Raman scattering microscopy. *Proc Natl Acad Sci USA*. 2015; 112:11624–11629. [PubMed: 26324899]
20. Ji M, Lewis S, Camelo-Piragua S, Ramkissoon SH, Snuderl M, Venneti S, Fisher-Hubbard A, Garrard M, Fu D, Wang AC, Heth JA, Maher CO, Sanai N, Johnson TD, Freudiger CW, Sagher O, Xie XS, Orringer DA. Detection of human brain tumor infiltration with quantitative stimulated Raman scattering microscopy. *Sci Transl Med*. 2015; 7:309ra163.
21. Fu D, Yu Y, Folick A, Currie E, Farese RV Jr, Tsai TH, Xie XS, Wang MC. In Vivo Metabolic Fingerprinting of Neutral Lipids with Hyperspectral Stimulated Raman Scattering Microscopy. *J Am Chem Soc*. 2014; 136:8820–8828. [PubMed: 24869754]
22. Fu D, Zhou J, Zhu WS, Manley PW, Wang YK, Hood T, Wylie A, Xie XS. Imaging the intracellular distribution of tyrosine kinase inhibitors in living cells with quantitative hyperspectral stimulated Raman scattering. *Nat Chem*. 2014; 6:614–622. [PubMed: 24950332]
23. Liu B, Lee HJ, Zhang D, Liao CS, Ji N, Xia Y, Cheng JX. Label-free spectroscopic detection of membrane potential using stimulated Raman scattering. *Applied Physics Letters*. 2015; 106:173704.
24. Lin-Vien, D., Colthup, NB., Fateley, WG., Grasselli, JG. *The Handbook of Infrared and Raman Characteristic Frequencies of Organic Molecules*. Academic Press; Cambridge, MA: 1991.
25. Ma J, Pazos IM, Zhang W, Culik RM, Gai F. Site-specific infrared probes of proteins. *Ann Rev Phys Chem*. 2015; 66:357–377. [PubMed: 25580624]
26. Fried SD, Boxer SG. Measuring electric fields and noncovalent interactions using the vibrational Stark effect. *Acc Chem Res*. 2015; 48:998–1006. [PubMed: 25799082]
27. Huang WE, Griffiths RI, Thompson IP, Bailey MJ, Whiteley AS. Raman microscopic analysis of single microbial cells. *Anal Chem*. 2004; 76:4452–4458. [PubMed: 15283587]
28. van Manen HJ, Lenferink A, Otto C. Noninvasive imaging of protein metabolic labeling in single human cells using stable isotopes and Raman microscopy. *Anal Chem*. 2008; 80:9576–9582. [PubMed: 19006335]
29. Yamakoshi H, Kosuke D, Masaya O, Jun A, Almar P, Katsumasa F, Satoshi K, Mikiko S. Imaging of EdU, an alkyne-tagged cell proliferation probe, by Raman microscopy. *J Am Chem Soc*. 2011; 133:6102–6105. [PubMed: 21443184]
30. Yamakoshi H, Dodo K, Palonpon A, Ando J, Fujita K, Kawata S, Sodeoka M. Alkyne-tag Raman imaging for visualization of mobile small molecules in live cells. *J Am Chem Soc*. 2012; 134:20681–20689. [PubMed: 23198907]
31. Lin L, Tian X, Hong S, Dai P, You Q, Wang R, Feng L, Xie C, Tian ZQ, Chen X. A bioorthogonal Raman reporter strategy for SERS detection of glycans on live cells. *Angew Chem Int Ed Engl*. 2013; 52:7266–7271. [PubMed: 23703791]
32. Prescher JA, Bertozzi CR. Chemistry in living systems. *Nat Chem Biol*. 2005; 1:13–21. [PubMed: 16407987]
33. Grammel M, Hang HC. Chemical reporters for biological discovery. *Nat Chem Biol*. 2013; 9:475–484. [PubMed: 23868317]
34. Beatty KE, Liu JC, Xie F, Dieterich DC, Schuman EM, Wang Q, Tirrell DA. Fluorescence visualization of newly synthesized proteins in mammalian cells. *Angew Chem*. 2006; 45:7364–7367. [PubMed: 17036290]
35. Jao CY, Salic A. Exploring RNA transcription and turnover in vivo by using click chemistry. *Proc Natl Acad Sci USA*. 2008; 105:15779–15784. [PubMed: 18840688]
36. Salic A, Mitchison TJ. A chemical method for fast and sensitive detection of DNA synthesis in vivo. *Proc Natl Acad Sci USA*. 2008; 105:2415–2420. [PubMed: 18272492]
37. Jao CY, Roth M, Welti R, Salic A. Metabolic labeling and direct imaging of choline phospholipids in vivo. *Proc Natl Acad Sci USA*. 2009; 106:15332–15337. [PubMed: 19706413]

38. Hang HC, Wilson JP, Charron G. Bioorthogonal chemical reporters for analyzing protein lipidation and lipid trafficking. *Acc Chem Res.* 2011; 44:699–708. [PubMed: 21675729]
39. Wei L, Hu F, Shen Y, Chen Z, Yu Y, Lin C, Wang MC, Min W. Live-cell imaging with alkyne-tagged small biomolecules by stimulated Raman Scattering. *Nature Methods.* 2014; 11:410–412. [PubMed: 24584195]
40. Hong S, Chen T, Zhu Y, Li A, Huang Y, Chen X. Live-cell stimulated Raman scattering imaging of alkyne-tagged biomolecules. *Angew Chem Int Ed.* 2014; 53:5827–5231.
41. Hu F, Chen Z, Zhang L, Shen Y, Wei L, Min W. Vibrational imaging of glucose uptake activity in live cells and tissues by stimulated Raman scattering. *Angew Chem Int Ed.* 2015; 54:9821–9825.
42. Lee HJ, Zhang W, Zhang D, Yang Y, Liu B, Barker EL, Buhman KK, Slipchenko LV, Dai M, Cheng JX. Assessing cholesterol storage in live cells and *C. elegans* by stimulated Raman scattering imaging of phenyl-Diyne cholesterol. *Sci Rep.* 2015; 5:7930. [PubMed: 25608867]
43. Chen Z, Paley D, Wei L, Weisman A, Friesner R, Nuckolls C, Min W. Multicolor live-cell chemical imaging by isotopically edited alkyne vibrational palette. *J Am Chem Soc.* 2014; 136:8027–8033. [PubMed: 24849912]
44. Zhang D, Slipchenko MN, Cheng J-X. Highly sensitive vibrational imaging by femtosecond pulse stimulated Raman loss. *J Phys Chem Lett.* 2011; 2:1248–1253. [PubMed: 21731798]
45. Wei L, Yu Y, Shen Y, Wang WC, Min W. Vibrational imaging of newly synthesized proteins in live cells by stimulated Raman scattering microscopy. *Proc Natl Acad Sci USA.* 2013; 110:11226–11231. [PubMed: 23798434]
46. Wei L, Shen Y, Xu F, Hu F, Harrington JK, Targoff KL, Min W. Imaging complex protein metabolism in live organisms by stimulated Raman scattering microscopy with isotope labeling. *ACS Chem Bio.* 2015; 10:901–908. [PubMed: 25560305]
47. Hu F, Wei L, Shen Y, Min W. Live-cell imaging of choline metabolites through stimulated Raman scattering coupled with isotope-based metabolic labeling. *Analyst.* 2014; 139:2312–2317. [PubMed: 24555181]
48. Li J, Cheng JX. Direct visualization of de novo lipogenesis in single living cells. *Sci Rep.* 2014; 4:6807. [PubMed: 25351207]
49. Alfonso-García A, Pfisterer SG, Riezman H, Ikonen E, Potma EO. D38-cholesterol as a Raman active probe for imaging intracellular cholesterol storage. *J Biomed Opt.* 2016; 21:61003. [PubMed: 26719944]
50. Shen Y, Xu F, Wei L, Hu F, Min W. Live-cell quantitative imaging of proteome degradation by stimulated Raman scattering. *Angew Chem Int Ed.* 2014; 53:5596–5599.
51. Baskin JM, Prescher JA, Laughlin ST, Agard NJ, Chang PV, Miller IA, Lo A, Codelli JA, Bertozzi CR. *Proc Natl Acad Sci USA.* 2007; 104:16793–16797. [PubMed: 17942682]
52. Ando J, Kinoshita M, Cui J, Yamakoshi H, Dodo K, Katsumasa F, Murata M, Sodeoka M. Sphingomyelin distribution in lipid rafts of artificial monolayer membranes visualized by Raman microscopy. *Proc Natl Acad Sci USA.* 2015; 112:4558–4563. [PubMed: 25825736]
53. Mullard, Asher. Deuterated drugs draw heavier backing. *Nat Rev Drug Discov.* 2016; 15:219–221. [PubMed: 27032821]
54. Hershey, JWB. Sonenberg, N., Mathews, MB., editors. Protein synthesis and translational control. Cold Spring Harbor Laboratory Press; 2012.
55. Martin KC, Barad M, Kandel ER. Local protein synthesis and its role in synapse-specific plasticity. *Curr Opin Neurobiol.* 2000; 10:587–592. [PubMed: 11084321]
56. Ong SE, Blagoev B, Kratchmarova I, Kristensen DB, Steen H, Pandey A, Mann M. Stable isotope labeling by amino acids in cell culture, SILAC, as a simple and accurate approach to expression proteomics. *Mol Cell Proteomics.* 2002; 1:376–386. [PubMed: 12118079]
57. Nag H, Venkata N, Shigeto S. Stable isotope-labeled Raman imaging reveals dynamic proteome localization to lipid droplets in single fission yeast cells. *Chem Biol.* 2012; 19:1373–1380. [PubMed: 23177192]
58. Goldberg AL. Protein degradation and protection against misfolded or damaged proteins. *Nature.* 2003; 426:895–899. [PubMed: 14685250]

59. Arrasate M, Mitra S, Schweitzer ES, Segal MR, Finkbeiner S. Inclusion body formation reduces levels of mutant huntingtin and the risk of neuronal death. *Nature*. 2004; 431:805–810. [PubMed: 15483602]
60. Zhang D-S, Piazza V, Perrin BJ, Rzadzinska AK, Poczatek JC, Wang M, Prosser HM, Ervasti JM, Corey DP, Lechene CP. Multi-isotope imaging mass spectrometry reveals slow protein turnover in hair-cell stereocilia. *Nature*. 2012; 481:520–524. [PubMed: 22246323]
61. Ozeki Y, Umemura W, Otsuka Y, Satoh S, Hashimoto H, Sumimura K, Nishizawa N, Fukui K, Itoh K. High-speed molecular spectral imaging of tissue with stimulated Raman scattering. *Nat Photonics*. 2012; 6:845–851.
62. Fu D, Holtom G, Freudiger C, Zhang X, Xie XS. Hyperspectral imaging with stimulated Raman scattering by chirped femtosecond lasers. *J Phys Chem B*. 2012; 117:4634–4640.
63. Zhang D, Wang P, Slipchenko MN, Cheng JX. Fast Vibrational Imaging of Single Cells and Tissues by Stimulated Raman Scattering Microscopy. *Acc Chem Res*. 2014; 47:2282–2290. [PubMed: 24871269]

## Biography

**Lu Wei** received her B.S. degree in Chemistry from Kuang Yaming Honors School, Nanjing University, China in 2010 and obtained her Ph. D in Chemistry from Columbia University in 2015. Lu is currently a postdoctoral research scientist at Columbia University. Her research focuses on developing novel nonlinear optical spectroscopy and microscopy and devising new optical bio-imaging schemes.

**Fanghao Hu** received his B.S. degree in Chemistry from Wuhan University and is currently a Ph.D. candidate at Columbia University. His research focuses on spectroscopic and chemical development for stimulated Raman scattering imaging in biochemical systems.

**Zhixing Chen** received his B.S. degree from Tsinghua University, China in 2008. After working as a research assistant in Peking University, he obtained his Ph. D in chemistry at Columbia University in 2014. Zhixing is currently a postdoctoral researcher at Stanford University. His research interests include novel synthetic chemistry toward small and macro molecules and their applications in the field of bio-imaging.

**Yihui Shen** received her B.S degree in Chemistry from Peking University in 2012. She is currently a Ph.D. candidate in Chemistry at Columbia University and a HHMI International Student Research Fellow. Her research focuses on applying microscopic imaging, including SRS and fluorescence, to provide new biophysical and biochemical insights into metabolic diseases.

**Luyuan Zhang** obtained her Ph. D in Chemical Physics in 2010 at The Ohio State University. She is currently a postdoctoral research scientist at Columbia University working on imaging abnormal metabolism in morbid animal models. Her research interests are in developing and applying novel nonlinear Raman microscopy for studies of various cellular activities.

**Wei Min** graduated from Peking University, China, with a Bachelor's degree in 2003. He received his Ph.D. in Chemistry from Harvard University in 2008 with Prof. Sunney Xie. After continuing his postdoctoral work in Xie group, Dr. Min joined the faculty of Department of Chemistry at Columbia University in July of 2010. Dr. Min is currently an

Associate Professor there, and his research interests focus on developing novel optical spectroscopy and microscopy technology to address biomedical problems.

Author Manuscript

Author Manuscript

Author Manuscript

Author Manuscript

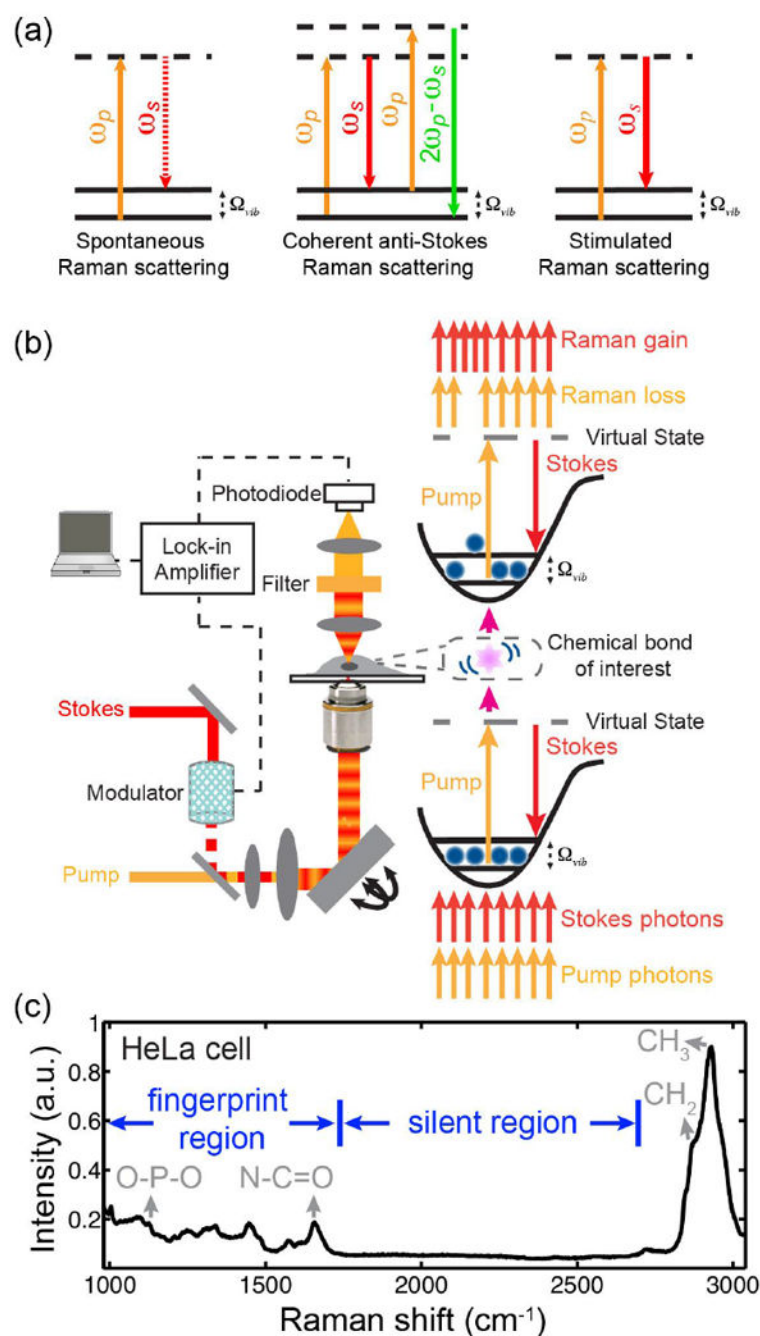


**Figure 1.** Physical principle and instrumental setup for stimulated Raman scattering microscopy. (a) Energy diagrams for spontaneous Raman scattering, coherent Anti-Stokes Raman scattering (CARS) and stimulated Raman scattering (SRS). (b) Experimental setup of typical SRS microscopy. (c) A Raman spectrum of mammalian cell samples designating the crowded fingerprint region and the cell-silent region.



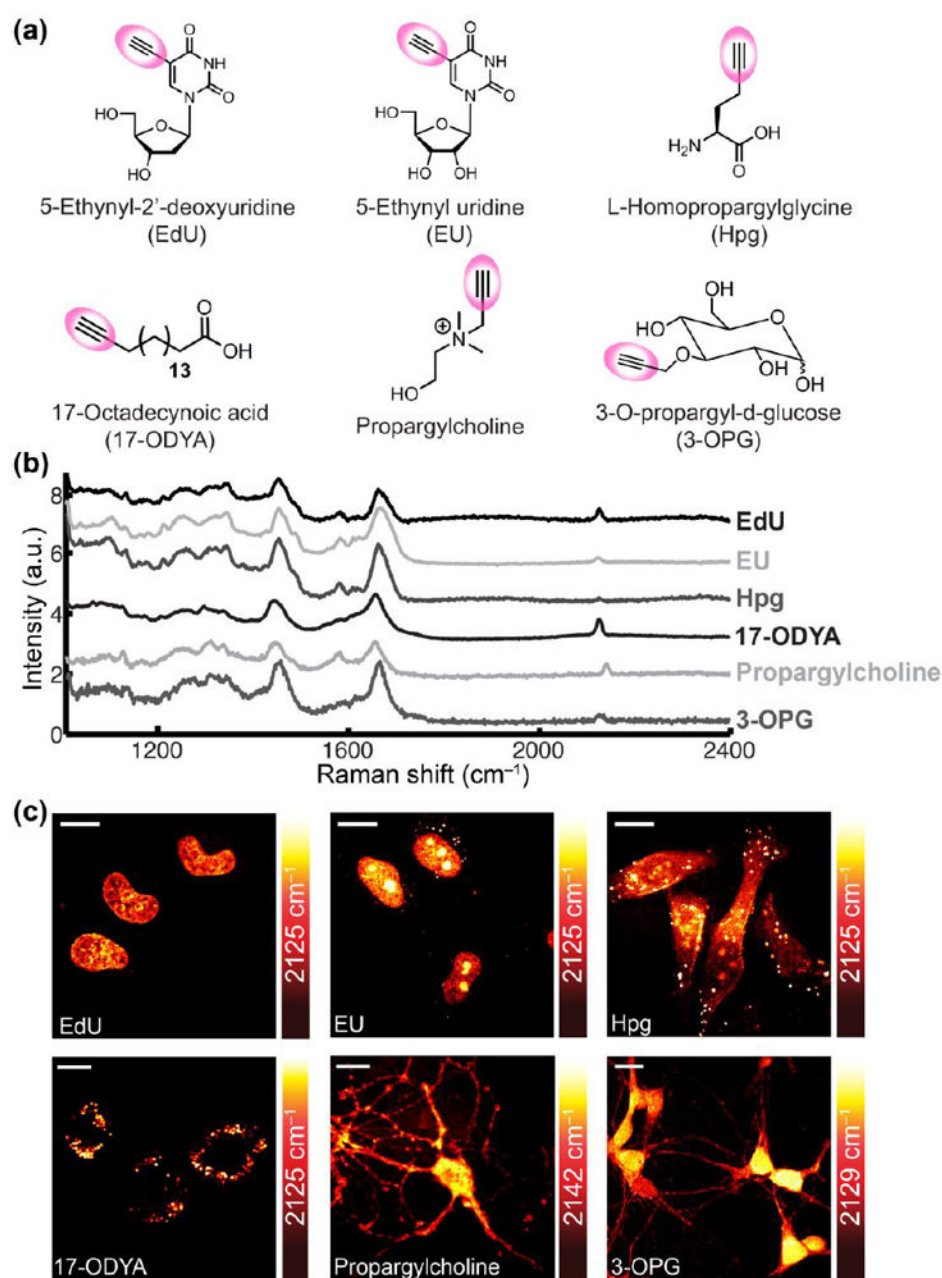


**Figure 2.** Sensitive and specific SRS imaging for diverse alkyne-bearing small biomolecules. (a) Chemical structures of alkyne-tagged small biomolecules. (b-c) The corresponding spontaneous Raman spectra (b) and the SRS images (c) of each alkyne-tagged small biomolecules after metabolic incorporation into mammalian cells or neurons. Adapted from refs. 39 and 41, copyrights 2014 Nature Publishing Group and 2015 John Wiley & Sons, Inc. Scale bar: 10  $\mu$ m.

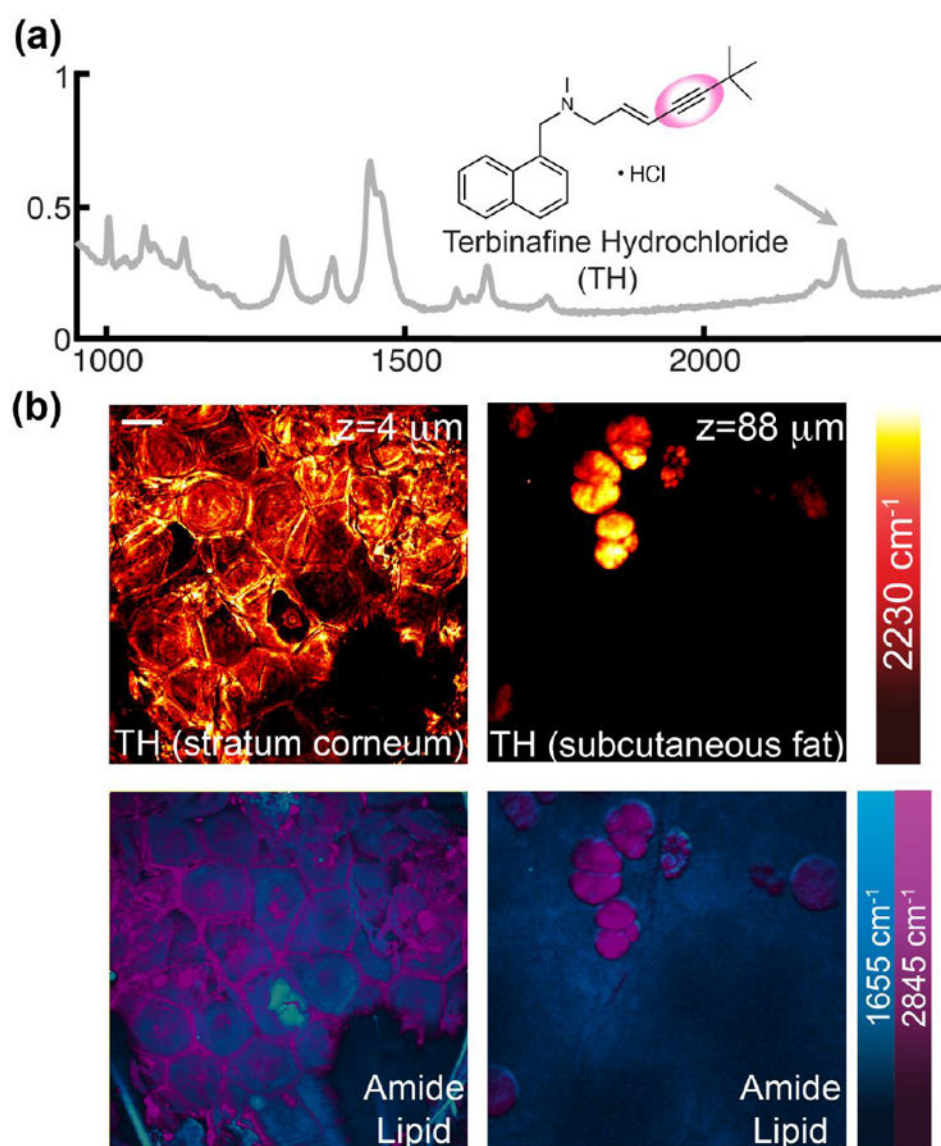


**Figure 3.** SRS imaging of *in vivo* delivery of an alkyne-bearing small-molecule drug, Terbinafine Hydrochloride (TH) into mouse ear. (a) Spontaneous Raman spectrum of TH. (b) SRS images at selected depths for TH at the alkyne channel and for proteins and lipids at respective label-free amide and lipid channels in mouse ear tissues. Adapted from ref. 39, copyright 2014 Nature Publishing Group. Scale bar: 20  $\mu\text{m}$ .

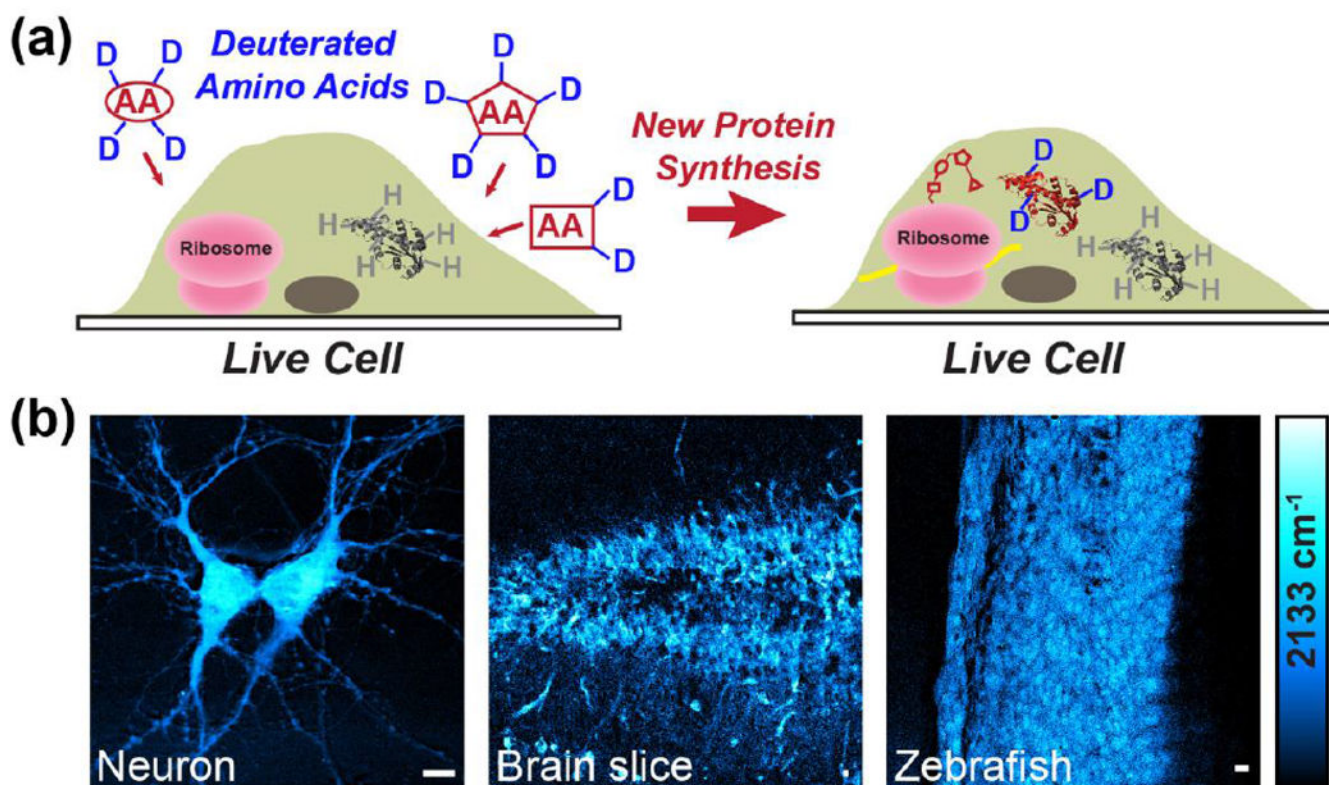


**Figure. 4.** SRS imaging of new protein synthesis by metabolic incorporation of deuterated amino acids (D-AAAs). a) A cartoon illustrating the metabolic enrichment of D-AAAs into cells' nascent proteins. b) SRS images of newly synthesized proteins in live neurons, brain slices and animals by targeting the C-D vibrational peak. Adapted from Ref. 46, copyright 2015 American Chemical Society. Scale bar: 10  $\mu$ m.

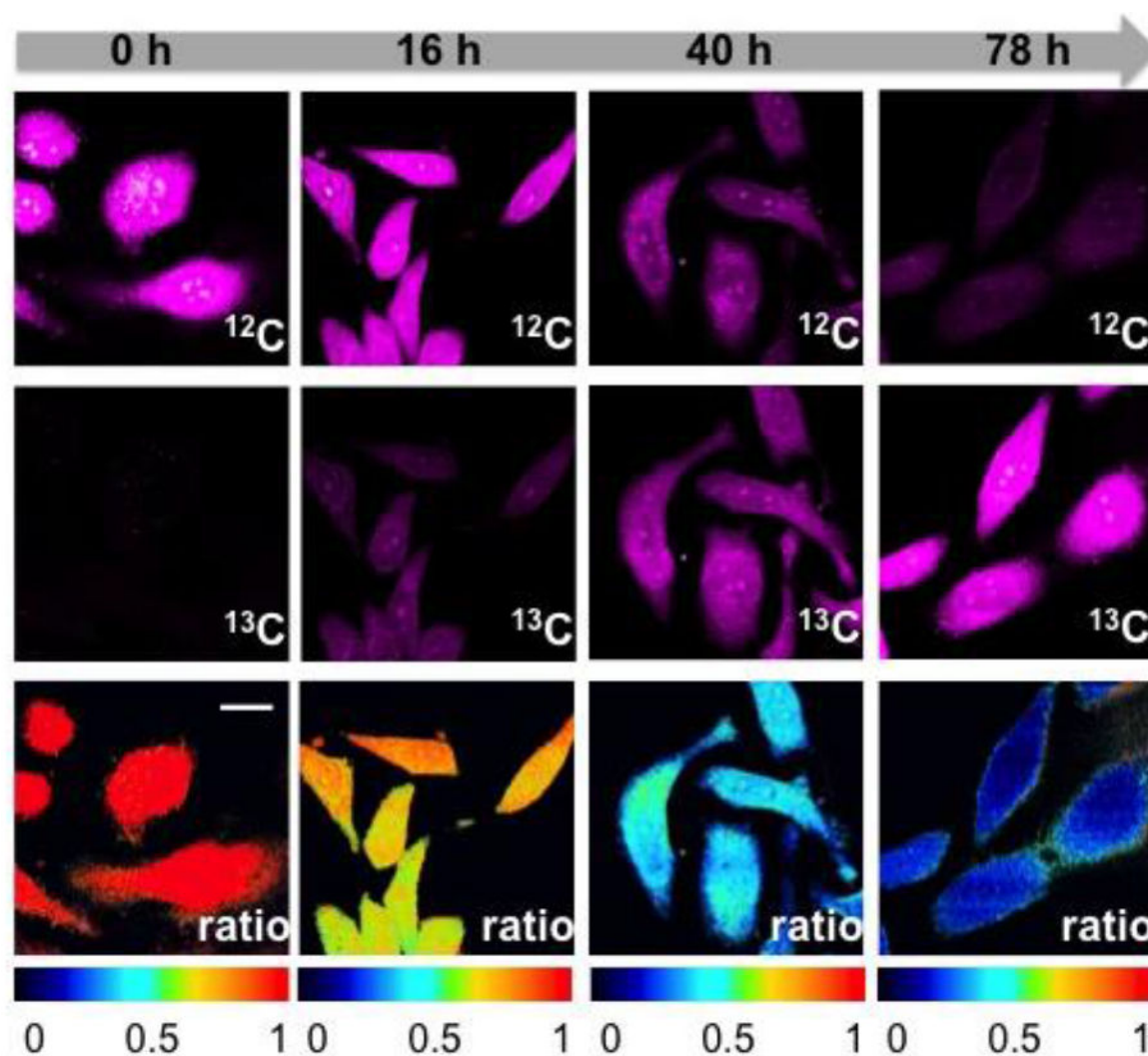


**Figure. 5.** SRS imaging of quantitative proteome degradation by metabolic incorporation of  $^{13}\text{C}$ -Phe. Time-dependent images at both  $^{12}\text{C}$ -Phe and  $^{13}\text{C}$ -Phe channels in live HeLa cells are obtained and the ratio maps of  $^{12}\text{C}/(^{12}\text{C}+^{13}\text{C})$  show quantitative decay of the pre-existing proteome. Adapted from Ref. 50, copyright 2015 John Wiley & Sons, Inc. Scale bar: 20  $\mu\text{m}$ .



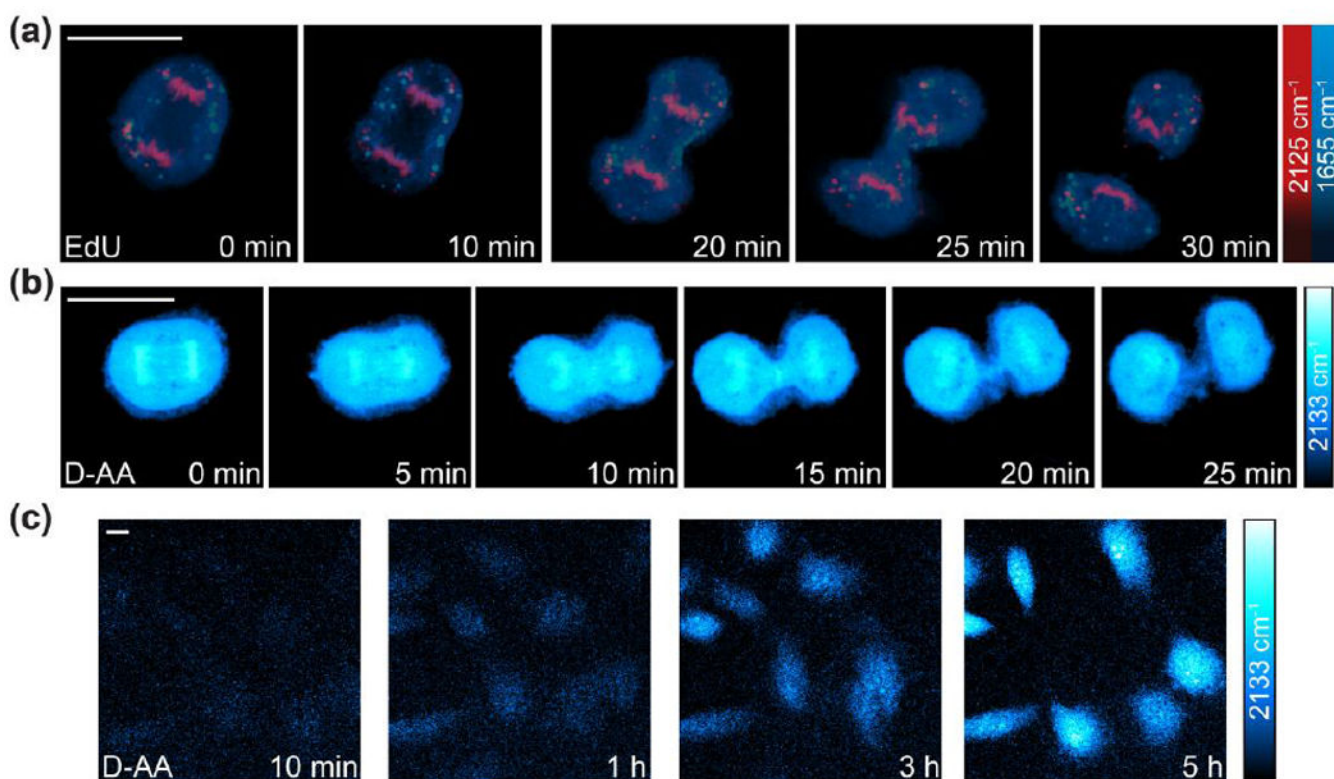


**Figure. 6.**

Bioorthogonal Chemical Imaging for the dynamic metabolism of small biomolecules. (a-b) Cell division tracking after incorporated with EdU for newly synthesized DNA (a) and D-AAAs for newly synthesized proteins (b). (a) is adapted from ref. 39, copyright 2014 Nature Publishing Group. (b) is adapted from Ref. 45, copyright 2013 National Academy of Sciences. (c) Time-lapse imaging from 10 min to 5 h for protein synthesis with metabolic labeling of D-AAAs. Adapted from Ref. 46, copyright 2015 American Chemical Society. Scale bar: 10  $\mu$ m.

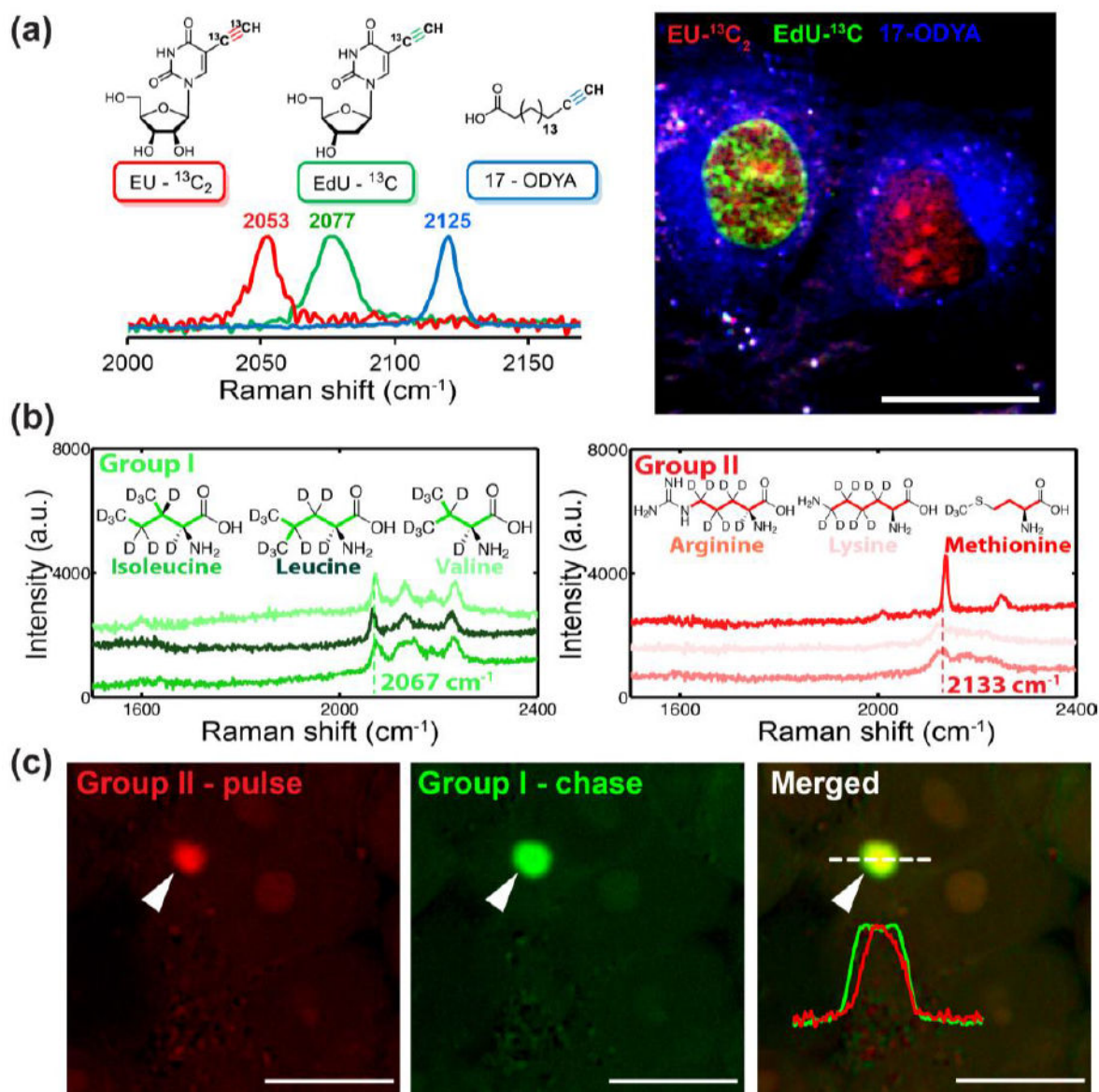


**Figure 7.**

Multicolor Bioorthogonal Chemical Imaging. (a) Multicolor SRS imaging of isotope-edited (EdU- $^{13}\text{C}$ , EU- $^{13}\text{C}_2$ ) and unedited (17-ODYA) alkyne-tagged small biomolecules after metabolic incorporation into new DNA (EdU- $^{13}\text{C}$ ), RNA (EU- $^{13}\text{C}_2$ ), and triglycerides (17-ODYA). Adapted from Ref. 43, copyright 2015 American Chemical Society. (b) Subgrouping of D-AAAs with similar chemical environments. (c) Two-color pulse-chase imaging for the protein aggregation formation of mutant Huntingtin proteins by metabolic labeling of two groups of D-AAAs. (b-c) adapted from Ref. 46, copyright 2015 American Chemical Society. Scale bar: 10  $\mu\text{m}$ .